Korean J. Chem. Eng., **29**(4), 540-548 (2012)
DOI: 10.1007/s11814-011-0200-8

Experimental and numerical investigation on the pyrolysis of single coarse lignite particles

Kai Zhang, Changfu You†, and Yulei Li

Key Laboratory for Thermal Science and Power Engineering of Ministry of Education,
Department of Thermal Engineering, Tsinghua University, Beijing 100084, China
(*Received 8 December 2010 • accepted 3 August 2011*)

Abstract–This paper reports on the mathematical modeling of the pyrolysis of single coarse lignite particles using a kinetics model coupled with a heat transfer model. The parallel reaction kinetics model of the lignite pyrolysis makes no assumptions about the activation energy distribution and the conversion of sub-reactions. The pyrolysis kinetics parameters were obtained on the basis of experimental data from thermogravimetric analysis (TGA) tests. The heat transfer model includes diffusive, convective and radiative heat transfer modes. The experimental investigations were carried out for single lignite particles in an electrically heated reactor. Measurements of the temperature and mass loss were performed during the pyrolysis in a nitrogen atmosphere. The model predictions for the temperature and mass loss histories agree well with the experimental data, verifying that the mathematical model accurately evaluates the pyrolysis of lignite particles. The effects of temperature and particle size on the pyrolysis time and final residual mass fraction were evaluated using the numerical model.

Key words: Lignite, Coarse Particle, Pyrolysis, Kinetics Model

INTRODUCTION

Lignite as a primary energy source will become increasingly important in energy supplies in the future because of its abundance, easy access and low mining costs. At the end of 2005, worldwide lignite reserves amounted to 207.4 billion tons and accounted for 17.7 percent of total coal resources [1]. The enormous resources of low-rank coal as an abundant fuel have become the focus of development for power generation [2-4]. Fluidized-bed combustion and gasification have been a recognized means of technology for power generation due to their inherent operating flexibility [5-7]. The use of low-rank coals is strongly dependent upon the behavior of the volatile matter, which can account for up to 50% of the specific energy for low rank coals. Thus, understanding of the volatile release is of paramount importance. However, pyrolysis and devolatilization, like other coal processing methods and coal properties, have been mainly investigated using finely pulverized (micrometer grain size) samples [8-14]. Larger, centimeter size coal particles have sometimes been considered, for example, in fluidized bed combustion studies, but the behavior of a single coal lump has rarely been investigated [15]. Small particles are likely to more quickly release the volatile matter, with very different release characteristics for the volatile matter in coarse particles because they are heated at a slower rate than the smaller particles [16-20].

Coarse particle coal pyrolysis is controlled by three main factors: the heat transfer to and within the coal particle, the chemical kinetics, and the mass transfer of the volatile species within the coal particle [21,22]. Several mathematical models have been developed to describe the devolatilization of coarse coal particles showing that the heat transfer and chemical kinetics dominate the overall reaction mechanism [21-23]. Koch et al. [24] suggested that the char layer which forms around the pyrolyzing coal particle provides no resistance to the out-flowing volatiles, while the data of Anthony et al. [25] indicated that the effect of pressure on the devolatilization of a Montana lignite is negligible. These results tend to support the assumption that the effect of mass transfer is negligible for low-rank coals, hence, it will not be considered in the current investigation.

The purpose of this work is to further advance the study of the pyrolysis mechanism of coarse coal particles (centimeter size) which are used in some gasification processes. A model was developed to predict the temperature response and the evolution of volatiles from coarse coal particles during pyrolysis. The model is based on the unsteady state heat conduction equation in spherical coordinates and uses a new parallel reaction model to predict the volatiles evolution. The model is validated with experimental results with simulation studies conducted to predict the pyrolysis behavior over a wide range of pyrolysis parameters and process conditions.

MATHEMATICAL MODEL

During pyrolysis, fine coal particles are generally assumed to be isothermal. The assumption of an isothermal particle requires that the heat transfer Biot number is less than 0.02. However, for coarse coal particle (>1 mm) with the larger Biot numbers, the internal temperature gradients must be considered [26,27]. Existing gas-solid heat transfer correlations and thermophysical properties can be used to show that the heat transfer Biot number varies from 1 to 20 for particle sizes >1 mm. Thus, modeling of the pyrolysis of coarse coal particles must consider heat transfer processes inside the particles. The heat transfer starts at the particle surface where the coal particle receives energy from the surrounding gas via convection and radiation heat transfer modes. The heat is subsequently transferred by conduction to the particle interior. Evolution of volatile

†To whom correspondence should be addressed.
E-mail: youcf@tsinghua.edu.cn
‡This work was presented at the 8th Kore-China Workshop on Clean Energy Technology held at Daejeon, Korea, Nov. 24-27, 2010.

matter from the coal particle therefore depends on the relative rates of convection and radiation heat transfer to the surface and conduction heat transfer into the interior. The loss of particle mass also creates a gas flow away from the particle, which is detrimental to the convection heat transfer.

The pyrolysis model for a coarse coal particle consists of a reaction kinetics model and a heat transfer model.

1. Kinetics Model

Many kinetics models have been reported for the pyrolysis of fine coal. There is the single kinetics rate model [8], the two competing rates model [9], the distributed activation energy model (DAEM) [10], the multiple parallel reaction model (MPRM) and others. Fine coal pyrolysis models have been reviewed by Saxena [11], Solomon et al. [12], Essenhigh [13] and Anthony and Howard [14]. The distributed activation energy model (DAEM) assumes a Gaussian activation energy distribution or sub reaction conversion of 0.58. The multiple parallel reaction model assumes a sub-reaction conversion of 0.632. However, there is no theoretical support for these assumptions of the activation energy distribution or the sub-reaction conversion.

This study presents a parallel reaction model to describe the pyrolysis kinetics without assumptions for the activation energy distribution and the conversion of sub-reaction. The model assumes that at each conversion only one first-order sub-reaction dominates the overall mass loss. Thus, at a given conversion of α^*, the ith sub reaction is the only reaction taking place at this conversion:

$$\frac{d\alpha}{dt} = A_i \exp\left(\frac{-E_i}{RT}\right)(1-\alpha) \tag{1}$$

where $\alpha = \dfrac{W_0 - W_t}{W_0 - W_\infty}$

Integrating Eq. (1), results in

$$1-\alpha^* \exp\left[-A_i \int_0^t \exp(-E_i/RT)dt\right] \tag{2}$$

If the conversion in two separate experiments at different heating rates, β_1 and β_2, is considered

$$\exp\left[-\frac{A_i}{\beta_1}\int_{T_0}^{T_1}\exp(-E_i/RT)dT\right] = \exp\left[-\frac{A_i}{\beta_2}\int_{T_0}^{T_2}\exp(-E_i/RT)dT\right] \tag{3}$$

Taking logarithms on each side yields

$$\frac{1}{\beta_1}\left[T_0\exp\left(\frac{-E_i}{RT_0}\right) - \frac{E_i}{R}\int_{E_i/RT_0}^{\infty}\frac{\exp(-u)}{u}du - T_1\exp\left(\frac{-E_i}{RT_1}\right) + \frac{E_i}{R}\int_{E_i/RT_1}^{\infty}\frac{\exp(-u)}{u}du\right] = \frac{1}{\beta_2}\left[T_0\exp\left(\frac{-E_i}{RT_0}\right) - \frac{E_i}{R}\int_{E_i/RT_0}^{\infty}\frac{\exp(-u)}{u}du - T_2\exp\left(\frac{-E_i}{RT_2}\right) + \frac{E_i}{R}\int_{E_i/RT_2}^{\infty}\frac{\exp(-u)}{u}du\right] \tag{4}$$

This is a nonlinear equation, which can be solved for the unknown E_i. Once E_i is known from Eq. (4), A_i can be calculated from

$$Ln(1-\alpha^*) = \frac{Ai}{\beta_1}\left[T_0\exp\left(\frac{-Ei}{RT_0}\right) - \frac{Ei}{R}\int_{Ei/RT_0}^{\infty}\frac{\exp(-u)}{u}du - T_1\exp\left(\frac{-Ei}{RT_1}\right) + \frac{Ei}{R}\int_{Ei/RT_1}^{\infty}\frac{\exp(-u)}{u}du\right] \tag{5}$$

Once each value of E and A is known, at each time:

$$M = 1-\alpha = \sum_{all\ reactions} f_i \exp\left[-A_i\int_0^t \exp(-E_i/RT)dt\right] \tag{6}$$

Where f_i is the contribution rate of the sub-reaction. Eq. (6) may be written as a matrix equation, where, for any set of temperatures T_0, T_1, T_2, etc., the mass of coal remaining, M(T), is given by

$$\begin{bmatrix} M(T_0) \\ M(T_1) \\ M(T_2) \\ . \\ . \\ . \end{bmatrix} = \begin{bmatrix} \psi_1(T_0) & \psi_2(T_0) & \cdots & \psi_n(T_0) \\ \psi_1(T_1) & \psi_2(T_1) & \cdots & \psi_n(T_1) \\ \psi_1(T_2) & \psi_2(T_2) & \cdots & \psi_n(T_2) \\ . & . & . & \\ . & . & . & \\ . & . & . & \end{bmatrix} \times \begin{bmatrix} f_1 \\ f_2 \\ . \\ . \\ f_n \end{bmatrix} \tag{7}$$

where $\psi_i(T) = \exp\left[-\dfrac{A_i}{\beta_1}\int_{T_0}^{T}\exp(-E_i/RT)dT\right]$

$$\frac{\partial \rho_s}{\partial t} = -\rho_{s0} V_\infty \frac{\partial M}{\partial t} \tag{8}$$

2. Heat Transfer Model

The convective heat transfer between the volatiles and the solids is incorporated into the governing equation. Using an infinitesimal

Table 1. Parameters used in the simulations

Parameter	Correlation/value	Source
C_{ps} ($J\cdot kg^{-1}\cdot K^{-1}$)	$C_{ps} = c_{P\_daf}w_{daf} + c_{P\_ash}w_{ash}$	[28]
C_{p_daf} ($J\cdot kg^{-1}\cdot K^{-1}$)	$443.5 + 1.036T + (11.862 + 7.1\times10^{-3}\,T)w_v$	[29]
C_{p_ash} ($J\cdot kg^{-1}\cdot K^{-1}$)	$752 + 0.293T$	[30]
λ_s ($W\cdot m^{-1}\cdot K^{-1}$)	$\left[\left(\dfrac{w_C}{1.47} + \dfrac{w_H}{0.0118}\right)\left(\dfrac{273}{T}\right)^{0.5}\right]^{-1}$	[31]
ε	0.95	
σ ($W\cdot m^{-2}\cdot K^{-4}$)	5.67×10^{-8}	
ΔH ($kJ\cdot kg^{-1}$)	300	
ρ_{s0_huo} ($kg\cdot m^{-3}$)	830	
ρ_{s0_hai} ($kg\cdot m^{-3}$)	850	

Table 2. Ultimate and proximate analyses of the raw lignite

Samples	Ultimate analysis (wt%)[a]					Proximate analysis (wt%)[a]			Proximate analysis (wt%)[b]
	C	H	O	N	S	V	FC	A	M
Huolinhe lignite	55.45	3.83	15.25	0.93	0.57	38.46	37.57	23.97	31.93
Hailaer lignite	50.97	2.98	13.88	0.82	0.62	35.72	33.55	30.73	28.87

[a]Dry basis

[b]As received basis

control volume in the radial direction of the solid particle, the energy balance equation in spherical coordinates is:

$$\frac{\partial}{\partial t}(\rho_s C_{ps} T) + \frac{\partial}{\partial r}(\rho_g C_{pg} T \cdot u_r) = \frac{1}{r^2}\frac{\partial}{\partial r}\left(\lambda_s r^2 \frac{\partial T}{\partial r}\right) - \Delta H\left(-\frac{\partial \rho_s}{\partial t}\right) \quad (9)$$

$$\text{where } u_r = \frac{\int_0^r 4\pi r^2 \frac{d\rho_s}{dt} dr}{4\pi r^2 \cdot \rho_g} \quad (10)$$

The initial and boundary conditions are

$$T|_{t=0} = T_0$$

$$\left.\frac{\partial T}{\partial r}\right|_{r=0} = 0$$

$$\lambda \left.\frac{\partial T}{\partial r}\right|_{r=R} = h(T_f - T) + \varepsilon\sigma(T_f^4 - T^4)$$

During pyrolysis the residual mass fraction is calculated on a dry sample basis and expressed as follows:

$$\text{residual mass fraction} = \frac{\text{sample weight at any pyrolysis time t}}{\text{initial dry sample weight}} \quad (11)$$

The parameters used in the model are listed in Table 1.

EXPERIMENT

1. Materials

The two kinds of Chinese lignite used in these experiments were

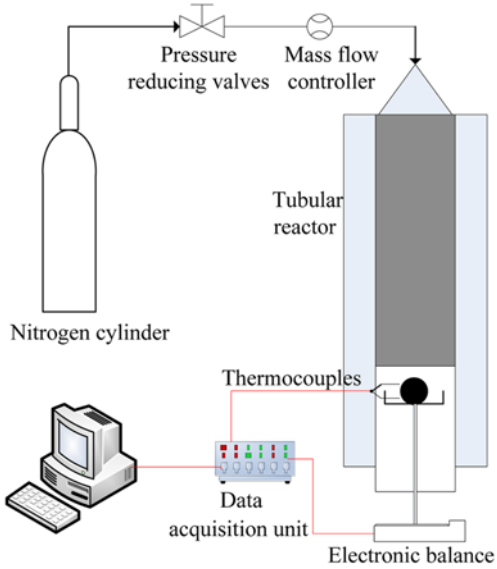

Fig. 1. Schematic diagram of the experimental system.

Table 3. Pyrolysis kinetic parameters of Hailaer lignite

N	E J/mol	A s-1	f /	N	E J/mol	A s-1	f /
1	138835.8	4.58E+12	0.045	26	289307.4	5.26E+17	0
2	99815.82	3.79E+07	0.012	27	299804.9	1.60E+18	0.020
3	109968.8	1.10E+08	0.050	28	308387.6	3.52E+18	0.028
4	139443.2	2.23E+10	0	29	318305.6	8.98E+18	0
5	179021.8	2.91E+13	0.011	30	328330.2	2.24E+19	0.040
6	198990.8	5.89E+14	0.034	31	334792.4	3.18E+19	0
7	213023	3.87E+15	0.001	32	346679.1	9.61E+19	0.036
8	219780.4	6.73E+15	0.042	33	357150.3	2.25E+20	0
9	228960.2	1.99E+16	0	34	369262.3	6.35E+20	0.040
10	229664.5	1.28E+16	0.020	35	383403	2.28E+21	0
11	230097	8.33E+15	0.040	36	398918.2	9.23E+21	0.033
12	229962.1	5.18E+15	0	37	417441.1	5.38E+22	0.010
13	229893.7	3.37E+15	0.001	38	436376.4	3.11E+23	0.019
14	229780.2	2.28E+15	0.062	39	456676.3	2.01E+24	0.027
15	232727.3	2.68E+15	0	40	465646.7	2.91E+24	0
16	238266.7	4.95E+15	0	41	438503.2	4.56E+22	0
17	239404.2	4.32E+15	0.036	42	386701.8	4.15E+19	0.006
18	242797.4	5.58E+15	0.032	43	401823.5	1.80E+20	0.091
19	247856.5	9.50E+15	0	44	438345.3	9.39E+21	0
20	248782.1	8.07E+15	0	45	488658	2.10E+24	0.035
21	253200.6	1.21E+16	0.042	46	519992.9	3.75E+25	0
22	258587.8	2.07E+16	0.030	47	549797.3	4.52E+26	0.050
23	259925.9	1.80E+16	0	48	582759.3	5.90E+27	0
24	271390.7	7.63E+16	0	49	739596.3	6.33E+27	0.060
25	278573.7	1.56E+17	0.047				

Huolinhe lignite and Hailaer lignite. The ultimate and proximate analyses of the raw lignite are listed in Table 2. Lignite fines in the size range of 97-125 μm were used to study the pyrolysis kinetics. The lignite lumps were dried at a temperature of 105 °C for at least 10 h before the pyrolysis experiments to remove moisture. Then the lignite lumps were ground into spherical particles (20 mm and 30 mm diameter) to facilitate comparison of the experimental and numerical results.

2. Thermogravimetric Experiments with Fine Grain Lignite

The thermogravimetric experiments were carried out in a TGA/Q600. The inert gas used for the pyrolysis was nitrogen with a flow rate of 100 ml/min. The initial mass of the samples was about 10 mg. Before the experiment was started, the furnace was purged for 30 minutes at room temperature. The furnace was then heated to 105 °C at a heating rate of 10 K/min and held at 105 °C for 10 minutes to evaporate external moisture. The furnace was subsequently heated from 105 °C to 900 °C at different heating rates (30 K/min, 50 K/min, 80 K/min, 100 K/min and 150 K/min) and held at this final temperature for 20 minutes.

3. Pyrolysis Experiment for a Single Coarse Lignite Particle

A schematic diagram of the pyrolysis experimental system for coarse lignite particles is shown in Fig. 1. The inside diameter of the tubular reactor was approximately 70 mm and the length was 1,400 mm. The tube was insulated by a thick layer of plaster of Paris around which heating wire was wound, forming the heating element of the reactor. The temperature around the particle was maintained at the desired value by the temperature control subsystem and measured by a K-type thermocouple with an accuracy of ±0.75%. An electrical single-pan balance was provided to continuously monitor the sample mass. The reactor was flushed continuously with inert nitrogen gas at a rate of 10 L/min inside the reactor. The flow rate was not high enough to interfere with the mass-loss measurement.

The temperatures at the center of the lignite sphere were measured during the pyrolysis by using K-type thermocouples. This type of thermocouple provides an accuracy of ±0.75% of the measured value. The electronic balance used to monitor the particle mass had an accuracy of ±0.1 mg. All experiments were performed at atmospheric pressure with the weights and temperatures recorded every 10 seconds. The electrical outputs for these two measurements were continuously logged by a data acquisition unit.

RESULTS AND DISCUSSION

1. Pyrolysis Reaction Kinetics Parameters

The kinetics parameters listed in Tables 3 and 4 were obtained using an established kinetics model and thermogravimetric experimental data at heating rates of 50 K/min and 100 K/min. Excluding sub-reactions with a distribution rate of 0, The Hailaer lignite kinetics model contains 30 sub-reactions, and the Huolinhe lignite kinetic model contains 24 sub-reactions. The calculated activation energies (E_i) were mainly in the range of 100-500 KJ/mol, with pre-exponential factors (A_i) of 10^7-10^{26} s^{-1}, which agree with the results

Table 4. Pyrolysis kinetic parameters of Huolinhe lignite

N	E J/mol	A s-1	f /	N	E J/mol	A s-1	f /
1	99479.08	5.55E+07	0.031	26	259963.8	2.93E+16	0
2	129642.8	2.67E+08	0.124	27	268417.4	9.38E+16	0
3	169459.9	2.51E+11	0	28	270957.4	1.12E+17	0.048
4	189448.3	5.69E+12	0	29	279578.3	3.40E+17	0.045
5	199403.2	2.27E+13	0	30	288983.8	1.12E+18	0
6	207353.2	6.99E+13	0	31	299799.7	4.28E+18	0
7	209902.3	8.53E+13	0	32	309921	1.38E+19	0.037
8	217773.4	2.84E+14	0.181	33	327436.9	1.27E+20	0
9	219227.1	3.07E+14	0	34	339563.5	4.68E+20	0.042
10	221672.2	4.02E+14	0	35	357443.3	3.75E+21	0.005
11	226303.7	7.87E+14	0.009	36	379341.5	4.78E+22	0.026
12	227538.2	8.54E+14	0	37	404489.2	8.50E+23	0.019
13	228525.1	8.93E+14	0	38	427211.9	9.08E+24	0.017
14	229445.1	9.24E+14	0	39	438943.1	1.82E+25	0.021
15	233078.6	1.53E+15	0	40	432525.6	2.75E+24	0.020
16	235698.5	2.12E+15	0	41	448919.3	9.10E+24	0.021
17	238016.7	2.79E+15	0	42	474162.6	8.48E+25	0.020
18	239288.2	3.06E+15	0	43	519414.1	8.64E+27	0.023
19	239760	2.93E+15	0	44	574172.2	1.29E+28	0.019
20	245960.2	7.31E+15	0.167	45	608332.3	1.63E+28	0.022
21	247876.2	8.81E+15	0	46	629355.3	9.95E+27	0.015
22	248774.1	8.93E+15	0	47	638067.3	6.56E+27	0.026
23	249846.7	9.22E+15	0	48	611455.2	1.45E+28	0.010
24	257049.8	2.58E+16	0	49	827055.9	3.07E+27	0.052
25	259087.1	3.04E+16	0				

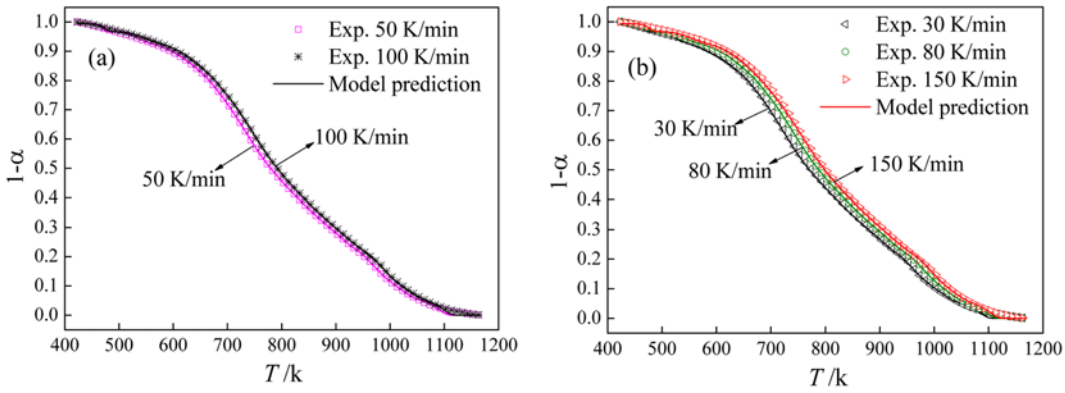

Fig. 2. Experimental data and model predictions for the normalized mass of Hailaer lignite: (a) β=50 k/min and 100 K/min; (b) β=30 k/min, 80 k/min and 150 K/min.

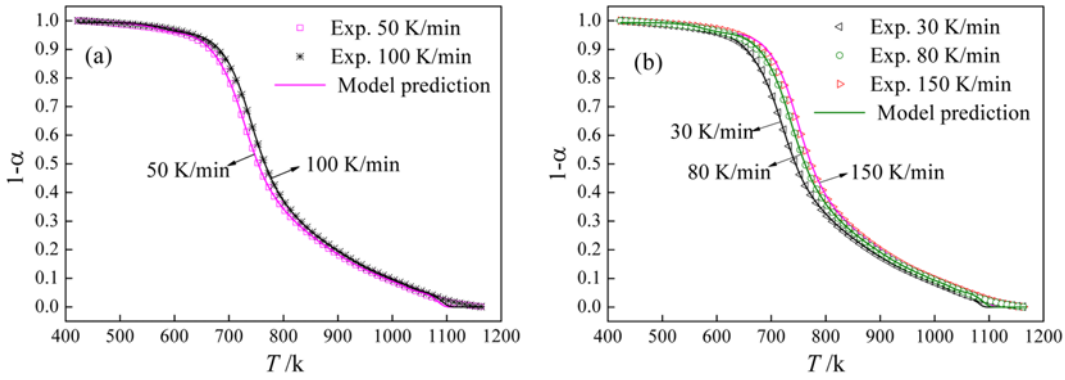

Fig. 3. Experimental data and model predictions for the normalized mass of Huolinhe lignite: (a) β=50 k/min and 100 K/min; (b) β=30 k/min, 80 k/min and 150 K/min.

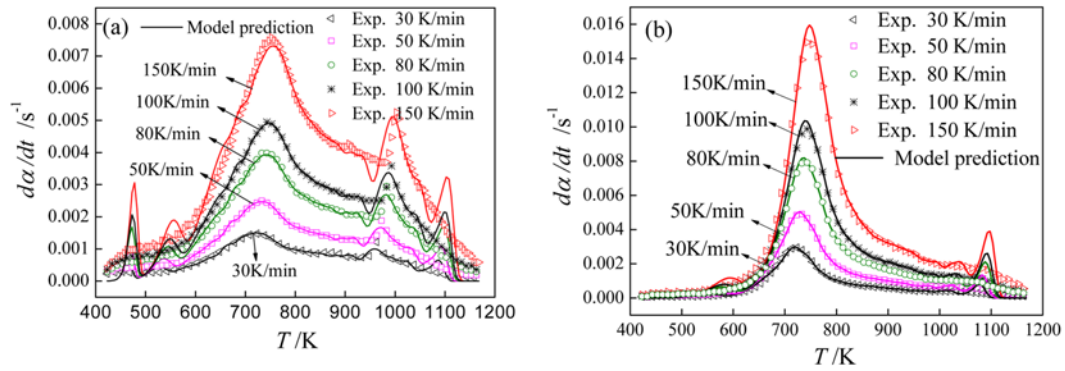

Fig. 4. Experimental data and model predictions for the pyrolysis rate: (a) Hailaer lignite; (b) Huolinhe lignite.

of Miura et al. [32,33] for coal pyrolysis kinetics.

The experimental and calculated results for the normalized mass and the pyrolysis rate profiles for Huolinhe fine lignite and Hailaer fine lignite are compared in Figs. 2, 3 and 4. The results show that the residual mass and the weight loss rate are accurately predicted.

2. Validation of the Pyrolysis Model for the Single Coarse Lignite Particles

The effects of internal convection arising from the volatiles evolution and the heat of reaction were investigated using four models: (1) with internal convection and without heat of reaction, (2) without internal convection and without the heat of reaction, (3) with internal convection and with the heat of reaction, and (4) without internal convection and with the heat of reaction. The results in Fig. 5 show that the predicted centre temperature is lower in the presence of heat of reaction since the pyrolysis reactions absorb heat from the particle. Fig. 5 also shows that the internal convection has only slight influence on lignite particle pyrolysis. The results in Fig. 6 show that the curves (with the heat of reaction) have better agreement with the experimental results for both the residual mass fraction profile and the center temperature profile. Thus, this investigation

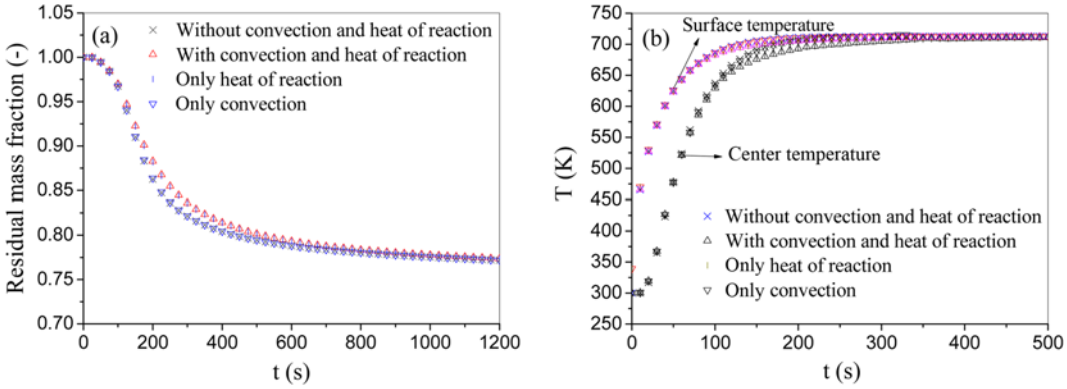

Fig. 5. Model comparison for Huolinhe lignite, T_f=713 K, D_0=20 mm: (a) Variations of the residual mass fraction; (b) Variations of particle temperature.

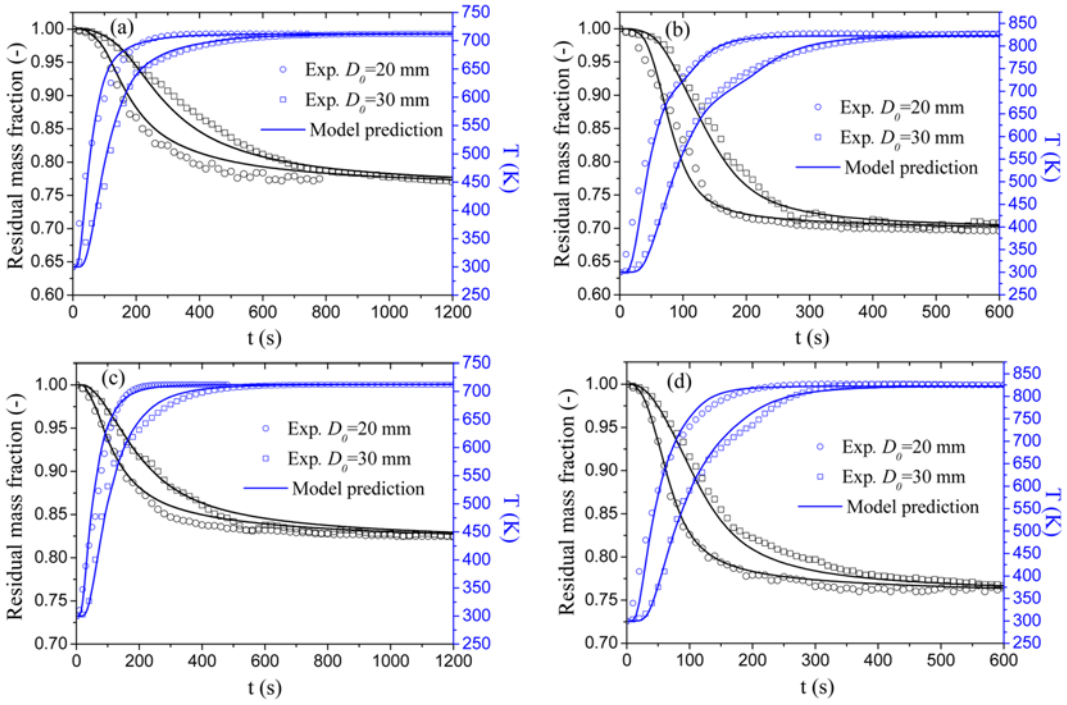

Fig. 6. Experimental data and model predictions for the residual mass fraction: (a) Huolinhe lignite, T_f=713 K; (b) Huolinhe lignite, T_f=823 K; (c) Hailaer lignite, T_f=713 K; (d) Hailaer lignite, T_f=823 K.

underlines the importance of incorporating the heat of reaction in the pyrolysis model.

The model has been validated with experimental results for large spherical lignite particles at temperatures of 713 and 823 K. Figs. 6(a) and 6(c) show the experimental and predicted center temperature and residual mass fraction profiles for Huolinhe and Hailaer lignite particles at 713 K. The agreement between the experimental data and model prediction is good with respect to both the residual mass fraction and center temperature. Figs. 6(b) and 6(d) show similar trends at 823 K. The results in Fig. 6 show that at the lower pyrolysis temperature the mass loss is more gradual while at the higher temperature the pyrolyzing particle loses mass rapidly and quickly reaches the final residual mass fraction. Thus, as the pyrolysis temperature increases, the time needed to attain a given conversion level decreases. The results also show that the final residual mass fraction decreases as the pyrolysis temperature increases.

3. Simulation Studies

Numerical simulation can provide a better way to acquire more detailed information inside the particle, which is difficult to measure but very important. The numerical results agree well with the experimental data, verifying that the mathematical model can evaluate the pyrolysis performance of lignite particles and obtain more detailed information inside the particle.

3-1. Effect of Particle Size and Pyrolysis Temperature

The effects of the pyrolysis conditions such as the particle size, the pyrolysis temperature on the pyrolysis process were evaluated using the numerical model. The influence of particle size on the residual mass fraction is shown in Figs. 7(a) and 7(c) for Huolinhe and Hailaer lignite particles. Nearly the same final residual mass fractions are obtained for all particle sizes at a given temperature,

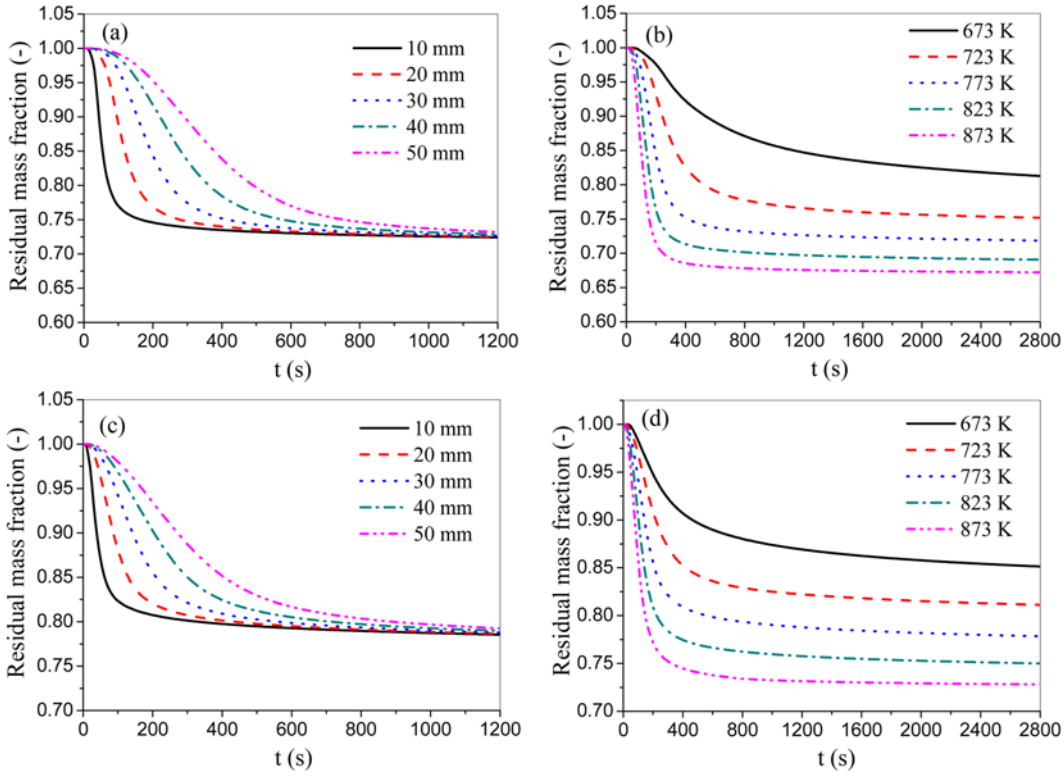

Fig. 7. Model predictions for the residual mass fraction: (a) Huolinhe lignite, T_f=773 K; (b) Huolinhe lignite, D_0=30 mm; (c) Hailaer lignite, T_f=773 K; (d) Hailaer lignite, D_0=30 mm.

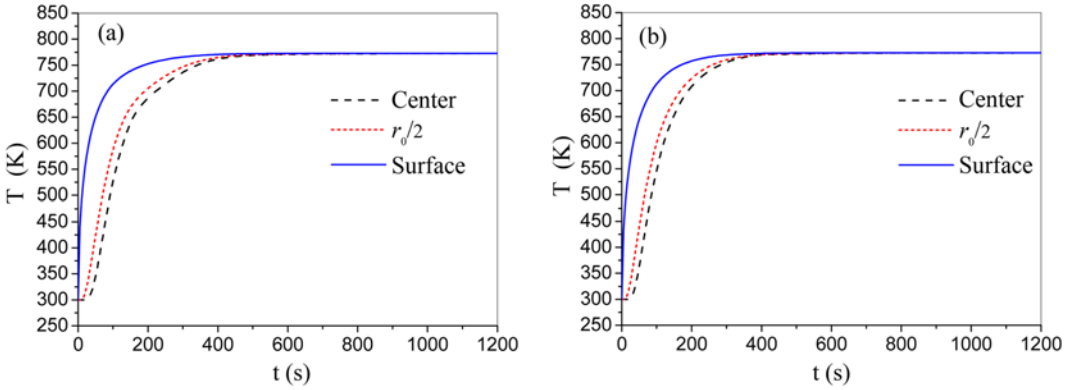

Fig. 8. Model predictions for the particle temperature: (a) Huolinhe lignite, T_f=773 K, D_0=30 mm; (b) Hailaer lignite, T_f=773 K, D_0= 30 mm.

which is the primary factor controlling the pyrolysis. However, the residue profiles over time differ for different particles, and the strong influence of sample size is readily observed with a more rapid decline in average mass with time for the 10 mm particle compared with the 20 mm, 30 mm, 40 mm, and 50 mm particles, since a smaller particle has a larger specific surface area for pyrolysis. The variation of the residual mass fraction with time is shown in Figs. 7(b) and 7(d) for different pyrolysis temperatures for Huolinhe and Hailaer lignite particles. These show that increasing pyrolysis temperatures reduces the pyrolysis time and a higher pyrolyzing temperature leads to a lower final residual mass fraction.

3-2. Profiles of Temperature and Residual Mass Fraction

The detailed information about temperature and the residual mass fraction inside the particles during the pyrolysis process was evaluated using the numerical model. Fig. 8 shows the simulated temperatures profiles at 773 K for pyrolysis of a lignite sphere with a 15 mm radius. When a particle is introduced into the reactor, the surface heats very quickly, depending on the convective heat transfer and the radiation flux. The center temperature is lower due to additional diffusion heat transfer resistance inside the particle. Fig. 8 also shows that the surface temperature reaches the bulk temperature after a significant length of time, which suggests that the external heat transfer resistance cannot be neglected for these particles. The results also show that the temperature at $r_0/2$ from the center always lies between the center and the surface temperatures.

Radial profiles of the residual mass fraction (Figs. 9(a) and 9(b))

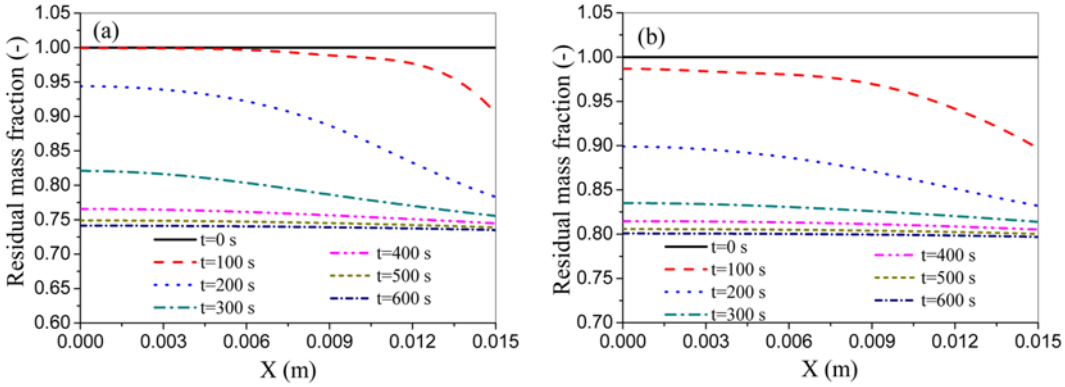

Fig. 9. Model predictions for the radial profile of the residual mass fraction: (a) Huolinhe lignite, T_f=773 K, D_0=30 mm; (b) Hailaer lignite, T_f=773 K, D_0=30 mm.

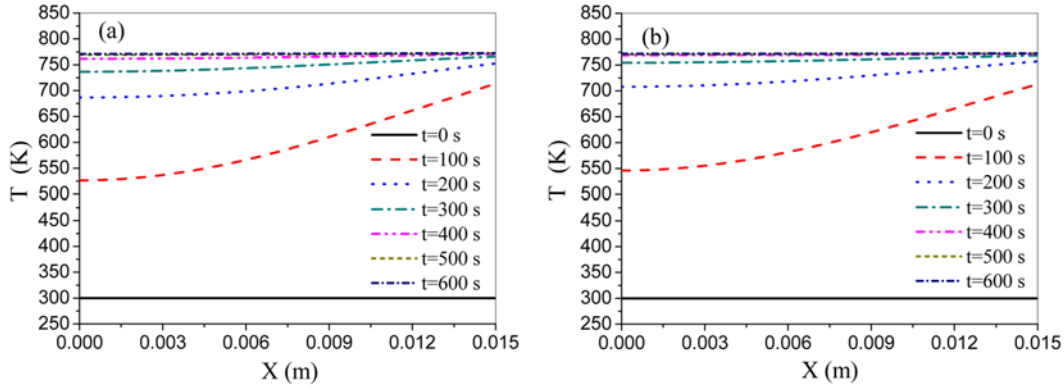

Fig. 10. Model predictions for the radial profile of the particle temperature: (a) Huolinhe lignite, T_f=773 K, D_0=30 mm; (b) Hailaer lignite, T_f=773 K, D_0=30 mm.

and particle temperature at 773 K (Figs. 10(a) and 10(b)) show the gradual heating and transformation of the lignite particle with a significant time lag for the reaction to start. These variations of the residual mass fraction in the particles are not well reported in the literature. During the pyrolysis, the outside temperature is higher than the inside temperature, so residual mass fraction at the surface is lower than at the center. A large residual mass fraction gradient appears in the particle for the pyrolysis process. Thus, the internal heat transfer resistance significantly affects the particle pyrolysis process. At higher temperature (773 K) the residual mass fraction profiles reveal that at the surface the lignite has already pyrolyzed and char is formed; at the center pyrolysis reaction is on progress, while the solid still contains a large amount of volatile matter. The residue profile is, however, almost flat at the completion of the reaction.

CONCLUSIONS

A mathematical model was developed to describe the pyrolysis of single coarse lignite particles using a kinetics model coupled with a heat transfer model. The parallel reaction kinetics model of the lignite pyrolysis makes no assumptions about the activation energy distribution and the conversion of sub-reactions. The kinetics parameters were then obtained from isothermal mass-loss studies of lignite fines in a TGA.

The effect of heat of reaction is found to be significant, while intra-particle convection has little influence on the lignite particle pyrolysis. Excellent agreement is found between the model prediction and the experimental data for two different lignites. The simulated temperature profiles show that the surface temperature reaches the bulk temperature after a very long period; thus, the external heat transfer resistance is quite important in the model. As the bulk temperatures increase, the final residual mass fraction decreases, which indicates higher volatile yields. At the same bulk temperature, the final residual mass fraction is not significantly affected by the particle size.

ACKNOWLEDGEMENTS

This research was supported by the National Natural Science Foundation of China (No. 51076083) and the Special Funds for Major State Basic Research Projects National 973 Project (No. 2006CB200305).

NOMENCLATURE

A : pre-exponential factor [s^{-1}]
C_{ps} : specific heat of dry coal [J kg^{-1} K^{-1}]
C_{p_daf} : specific heat of dry, ash-free coal [g]
C_{p_ash} : specific heat of coal ash [g]
D_0 : lignite particle diameter [mm]
E : activation energy [J mol^{-1}]

f : contribution rate of sub-reaction [dimensionless]
R : ideal gas constant [J mol^{-1} K^{-1}]
t : time [s]
T : temperature [K]
T_f : pyrolysis temperature [K]
w_{daf} : mass fraction of dry, ash-free coal in dry coal [dimensionless]
w_{ash} : mass fraction of coal ash in dry coal [dimensionless]
w_v : mass fraction of volatile matter in dry coal [dimensionless]
w_C : mass fraction of carbon in dry coal [dimensionless]
w_H : mass fraction of hydrogen in dry coal [dimensionless]
W_0 : fine coal weight after drying [mg]
W_t : weight at time t [mg]
W_∞ : final weight of fine coal [mg]
ΔH : heat of reaction [kJ kg^{-1}]

Greek Letters

α : conversion [dimensionless]
$1-\alpha$: normalized mass [dimensionless]
$d\alpha/dt$: pyrolysis rate [s^{-1}]
β : heating rate [K/min]
ε : emissivity coefficient [dimensionless]
λ : thermal conductivity [J m^{-1} s^{-1} K^{-1}]
ρ : density [kg m^{-3}]
σ : Stefan-Boltzmann constant [J m^{-2} s^{-1} K^{-4}]

Subscripts

ash : coal ash
daf : dry ash-free basis
hai : Hailaer lignite
huo : Huolinhe lignite

REFERENCES

1. T. Thomas, S. J. Sandro and G. Peter, *Int. J. Coal Geol.*, **72**, 1 (2007).
2. S. Z. Sun, J. W. Zhang, X. D. Hu, P. H. Qiou, J. Qian and Y. K. Qin, *Korean J. Chem. Eng.*, **26**, 554 (2009).
3. J. M. Lee, D. W. Kim and J. S. Kim, *Korean J. Chem. Eng.*, **26**, 506 (2009).
4. Y. J. Huang, B. S. Jin, Z. P. Zhong, R. Xiao and H. C. Zhong, *Korean J. Chem. Eng.*, **24**, 698 (2007).
5. J. W. Zhang, S. Z. Sun, X. D. Hu, R. Sun and Y. K. Qin, *Energy Fuels*, **23**, 2376 (2009).
6. F. Fang, Z. S. Li and N. S. Cai, *Korean J. Chem. Eng.*, **26**, 1414 (2009).
7. C. Prompubess, L. Mekasut, P. Piumsomboon and P. Kuchontara, *Korean J. Chem. Eng.*, **24**, 989 (2007).
8. S. Badzioch and P. G. Hawksley, *Ind. Eng. Chem. Proc. Des. Dev.*, **9**, 521 (1970).
9. H. Kobayashi, J. B. Howard and A. F. Sarofim, *Sixteenth symposium (international) on combustion*, Cambridge, U.K. (1976).
10. D. B. Anthony and J. B. Howard, *AIChE J.*, **22**, 625 (1976).
11. S. C. Saxena, *Prog. Energy Combust. Sci.*, **16**, 55 (1990).
12. R. P. Solomon, M. A. Serio and E. M. Suuberg, *Prog. Energy Combust. Sci.*, **18**, 133 (1992).
13. R. H. Essenhigh, *Chemistry of coal utilization*, John Wiley & Sons Inc., New York (1981).
14. D. B. Anthony, J. B. Howard, H. C. Hottel and H. P. Meissuer, *Fuel*, **55**, 121 (1976).
15. A. K. Sadhukhan, P. Gupta and R. K. Saha, *J. Anal. Appl. Pyrol.*, **81**, 183 (2008).
16. A. K. Sadhukhan, P. Gupta and R. K. Saha, *Bioresour. Technol.*, **100**, 3134 (2009).
17. J. Larfeldt, B. Leckner and M. C. Melaaen1, *Fuel*, **79**, 1637 (2000).
18. C. A. Heidenreich, H. M. Yan and D. K. Zhang, *Fuel*, **78**, 557 (1999).
19. J. S. Chern and A. N. Hayhurst, *Combust. Flame*, **157**, 925 (2010).
20. W. C. Park, A. Atreya and H. R. Baumb, *Combust. Flame*, **157**, 481 (2010).
21. P. K. Agarwal, W. E. Genetti and Y. Y. Lee, *Fuel*, **63**, 1157 (1984).
22. J. F. Stubington and K. Sumaryono, *Fuel*, **63**, 1013 (1984).
23. J. Tomeczek and J. Kowol, *Can. J. Chem. Eng.*, **69**, 286 (1990).
24. E. Koch, H. Juntgen and W. Peters, *Brennstoff Chemie*, **50**, 366 (1969).
25. D. B. Anthony, J. B. Howard, H. C. Hottel and H. P. Meissner, *Fifteenth symposium (international) on combustion*, Tokyo, Japan (1974).
26. B. A. Adesanya and H. N. Pham, *Fuel*, **74**, 896 (1995).
27. Y. Zhao, M. A. Serio and P. R. Solomon, *Twenty-Sixth symposium (international) on combustion*, Naples, Italy (1996).
28. D. Merrick, *Fuel*, **62**, 540 (1983).
29. V. Strezov, J. A. Lucas, T. J. Evans and L. Strezov, *J. Therm. Anal. Calorim.*, **78**, 385 (2004).
30. F. Hanrot, D. Ablitzer, J. L. Houzelot and M. Dirand, *Fuel*, **73**, 305 (1994).
31. A. Volborth, *Coal science and chemistry*, Elsevier, Amsterdam (1987).
32. K. Miura and T. Maki, *Energy Fuels*, **12**, 864 (1998).
33. K. Miura, *Energy Fuels*, **9**, 302 (1995).